

Nanoscale

Accepted Manuscript



This is an *Accepted Manuscript*, which has been through the Royal Society of Chemistry peer review process and has been accepted for publication.

Accepted Manuscripts are published online shortly after acceptance, before technical editing, formatting and proof reading. Using this free service, authors can make their results available to the community, in citable form, before we publish the edited article. We will replace this *Accepted Manuscript* with the edited and formatted *Advance Article* as soon as it is available.

You can find more information about *Accepted Manuscripts* in the [Information for Authors](#).

Please note that technical editing may introduce minor changes to the text and/or graphics, which may alter content. The journal's standard [Terms & Conditions](#) and the [Ethical guidelines](#) still apply. In no event shall the Royal Society of Chemistry be held responsible for any errors or omissions in this *Accepted Manuscript* or any consequences arising from the use of any information it contains.



3D Assembly of Silica encapsulated Semiconductor Nanocrystals

Christin Rengers^a, Sergei V. Voitekhovich^b, Susann Kittler^a, André Wolf^a, Marion Adam^c, Nikolai Gaponik^{a*}, Stefan Kaskel^c and Alexander Eychmüller^a

Received 00th January 20xx,
Accepted 00th January 20xx

DOI: 10.1039/x0xx00000x

www.rsc.org/

Non-ordered porous networks, so-called aerogels, can be achieved by the 3D assembly of quantum dots (QDs). These materials are well suited for photonic applications, however a certain quenching of the photoluminescence (PL) intensity is observed in these structures. This PL quenching is mainly attributed to energy transfer mechanisms that result from the close contact of the nanoparticles in the network. Here, we show the formation of a novel aerogel material with no quenching PL behavior by non-classical, reversible gel formation from tetrazole capped silica encapsulated QDs. Monitoring of the gelation/degelation by optical spectroscopy showed that the optical properties of the nanocrystals could be preserved in the 3D network since no spectral shifts and lifetime shortening, which can be attributed to the coupling between QDs, are observed in the gels as compared to the original colloidal solutions. In comparison to other silica monoliths, QDs in our gels are homogeneously distributed with a distinct and controllable distance. In addition we show that the silica shell is porous and allows metal ions to pass through the shell and interact with the QD core causing detectable changes of the emission properties. We further show the applicability of this gelation method to other QD materials which sets the stage for facile preparation of a variety of mixed gel structures.

Introduction

Non-ordered porous networks, so-called aerogels, are fine inorganic superstructures with enormously high porosity and inner surface area, resulting in densities as low as 3 times that of air.¹ These materials offer a wide variety of applications, e.g. in the field of catalysis,¹ due to their attractive catalytic, thermoresistant, piezoelectric, antiseptic, and many other properties, originating from the combination of the specific properties of nanoparticles by macroscale self-assembly.

In the early 1930s, the first synthesis of aerogels made from metal oxides was reported by Kistler² and was further developed starting from the late 1960s.^{1,3} So far, the most investigated aerogel materials are silica or metal oxides as well as their mixtures. But recently, creating aerogels from noble metal nanoparticles, colloidal quantum dots (QDs) or mixtures of both has attracted interest, since these materials may open opportunities in areas such as semiconductor technology, photocatalysis, optoelectronics, and photonics.⁴⁻¹² In 2005, Brock et al. first reported on CdS and CdSe nanocrystal aerogels.¹³ In order to perform gel formation, they had to transfer the non-polar organic stabilized QDs into polar organic or aqueous media. Later in 2008, our group developed a

photochemical treatment to create aerogels from thiol-capped CdTe nanocrystals, directly synthesized in water^{12,14} and a reversible gelation procedure for tetrazole-capped CdTe nanocrystals in 2010.¹⁵ Although the typical emission properties of the initial quantum confined nanocrystal building blocks could be preserved, usually in these structures a certain quenching of the photoluminescence (PL) intensity is observed compared to the colloidal solutions of the nanoparticles. This PL quenching is mainly attributed to energy transfer mechanisms that result from the close contact of the nanoparticles in the network. Introducing a spacer into the network and thus increasing the distance between the nanoparticles to a certain value may be a possibility to avoid this quenching behaviour.^{5,15} For this purpose, applying a dielectric shell of several nm thickness on fluorescent QDs, consisting of silica or polymers (e.g. polystyrene), might be an option to overcome this problem.

Thus far, silica coating of inorganic nanocrystals has been under investigation¹⁶⁻²¹ and the preparation methods can be classified in two approaches, i.e. the Stöber^{19,22} method and the reverse microemulsion technique²³⁻²⁵. Both approaches are usually causing a drop of the PL of the QDs. Only recently, modifications of the Stöber method allowing the retention or even an enhancement of the PL were reported.^{26,27} However, aiming for shell thicknesses of only several nanometers, it seems to be more promising to use the reverse microemulsion approach since it allows for better control of the particle size distribution for small sizes (from 20 nm to 150 nm) in comparison to the Stöber method.^{28,29}

^a Physical Chemistry, TU Dresden, Bergstr. 66b, 01062, Germany

^b Research Institute for Physical Chemical Problems, Belarusian State University, Leningradskaya Str. 14, 220030 Minsk, Belarus

^c Inorganic Chemistry I, TU Dresden, Bergstr. 66, 01062, Germany

Electronic Supplementary Information (ESI) available: See

DOI: 10.1039/x0xx00000x

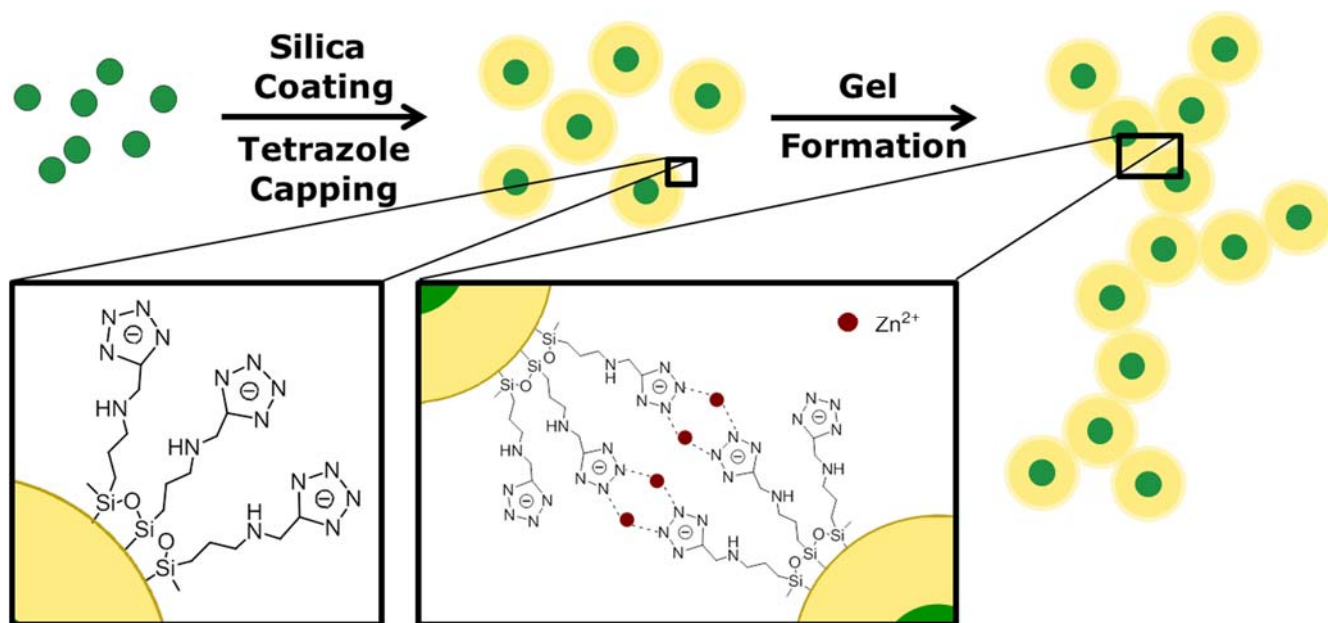


Figure 1: Schematic pathway of luminescent silica gel formation. In the first step organic synthesized CdSe/CdS core/shell QDs are covered with a silica shell using reversed microemulsion technique. After coating with a specially designed tetrazole ligand, the hydrogel is formed by metal ion assisted complexation in the second step. Subsequently, the aerogel can be achieved by supercritical point drying.

So far, in order to produce assembled structures, QDs were incorporated into silica matrix as a film or monolithic item. Thereby, QD composites were derived by surface exchange using organofunctional alkoxy silanes followed by a sol-gel process.^{26–31}

In this article, we show the formation of hydrogels and aerogels from silica encapsulated QDs, following a procedure reported earlier by our group.¹⁵ In comparison to other QD-silica monoliths, our gel is not derived via a sol-gel process but through interconnection of silica-QD nanoparticles leading to a homogeneous distribution of the QDs in the whole structure with a distinct and controllable distance to each other. Therefore, the silica coated QDs were functionalized with a tetrazole ligand specially designed to bind to the silica surface that allows for a controlled gel formation by interconnection of the negatively charged tetrazole rings through complexation with metal ions. This process is reversible and dissolution of the hydrogel can be achieved by the addition of a stronger complexant, e.g. EDTA that removes the metal ions from the network. Furthermore, we show monitoring of the gelation/degelation by optical spectroscopy, i.e. absorption and PL spectroscopy as well as PL lifetime and PL quantum yield (QY) measurement. These studies show that we were able to create a novel aerogel material with non-quenching PL behaviour, since no spectral shifts and lifetime shortening, which can be attributed to the coupling between QDs, are observed in gels as compared to the original colloidal solutions. Furthermore we show that the silica shell is not densely packed but rather porous and allows metal ions to pass through the shell and interact with the QD core.

Experimental

Chemicals and apparatus: All chemicals used were of analytical grade or of the highest purity available. All aqueous solutions were prepared from Milli-Q water (Millipore).

Synthesis of tetrazole capped silica encapsulated QDs: The silica encapsulation procedure was adopted from literature.³² In detail, in a 500 mL round bottom flask, 2.4 mL of IGEPA[®] CO-520 were added to 40 mL of anhydrous cyclohexane, followed by vigorous stirring for 15 min. Meanwhile, organic capped QDs ($2 \cdot 10^{-9}$ mol) were precipitated by addition of 1 mL of acetone and centrifugation at 4000 RPM for 3 min. The precipitate was dissolved in 1 mL of cyclohexane and then added to the stirred IGEPA solution. After 15 min of stirring, TEOS was added. In order to obtain 20 nm sized silica particles 15 μ L of TEOS were used. Higher amounts of TEOS resulted in larger particles. Finally, after 30 min of stirring, 280 μ L of ammonium hydroxide (28% in water) were slowly added and the mixture stirred for 48 h at RT in the sealed flask. Purification was done by mixing with 50 mL of ethanol and centrifugation at 5100 RPM for 30 min at 10 $^{\circ}$ C. The supernatant was discarded and the process repeated twice from pure ethanol. The particles were then redispersed in 1 mL of 4 mM NaOH aqueous solution. The solution was sonicated for 1 min and centrifuged at 2500 RPM for 3 min in order to remove any aggregates. The supernatant containing QD

encapsulated by silica shells was stored at 4 °C. Tetrazole capping was performed as following. In 200 μl of aqueous silica-QD solution a spatula tip of solid $(\text{MeO})_3\text{Si}-(\text{CH}_2)_3-\text{NH}-\text{CH}_2-\text{CN}_4\text{H}$ was dissolved. Under this condition, the ligand will immediately grow onto the silica surface resulting in flocculation. Addition of a few drops of 1 M NaOH led to a clear, stable solution, since tetrazole rings were deprotonated which allows charge stabilization of the silica particles.

Preparation of hydrogels from tetrazole capped silica encapsulated QDs and their degelation: Hydrogels were obtained by the stepwise addition of $\text{Zn}(\text{OAc})_2$ aqueous solution (10^{-2} M) to the tetrazole capped silica-QD colloidal solution up to complete gelation of the nanoparticles. The hydrogels were redissolved back into their colloidal form by the addition of an aliquot of 10^{-2} M ethylenediaminetetraacetic acid (EDTA) aqueous solution (adjusted to pH 12 by the addition of 1 M NaOH) equal to the Zn^{2+} concentration in the gelled sample. The gelation process has been monitored directly in a quartz cuvette with a light path of 10 mm by the stepwise addition of $\text{Zn}(\text{OAc})_2$ solution into the diluted silica-QD colloid with subsequent measurement of the absorbance, PL and PL lifetime.

Preparation of aerogels from hydrogels: A critical point drier (13200J-AB from Spi Supplies) was used for supercritical CO_2 drying to prevent the fine nanostructures from collapsing and to obtain self-supporting aerogel monoliths. This drying technique has been described previously.¹² In Brief, Acetone was added in small portions to the hydrogel and the resulting water/acetone mixture was removed a few times to assure that most of the water was exchanged with acetone. Subsequently, the sample was placed in a vacuum desiccator with 100% acetone containing some anhydrous CaCl_2 . The desiccator was evacuated until the acetone boils, sealed under low pressure, and left at these conditions for ca. 20 h. The procedure provides a very efficient but yet gentle exchange of the remaining water with acetone.

Characterization: UV-/Vis absorption spectra were acquired using a Cary 50 spectrophotometer (Varian Inc.) and a Cary 5000 spectrophotometer (Varian Inc.) with integrating sphere. PL measurements were recorded using a FluoroMax-4 spectrofluorimeter (HORIBA Jobin Yvon Inc.). PL lifetime measurements were performed on a Fluorolog-3 spectrofluorimeter (HORIBA Jobin Yvon Inc.) equipped with a 200 ps pulsed LED diode emitting at 403 nm and a TCSPC module. All measurements were performed at room temperature. PL QY of colloidal solutions was determined in reference to rhodamine 6g and rhodamine 101. For scattering samples, absolute PL QY were measured using a Fluorolog-3 spectrofluorimeter (HORIBA Jobin Yvon Inc.) equipped with a Quanta- ϕ integrating sphere.

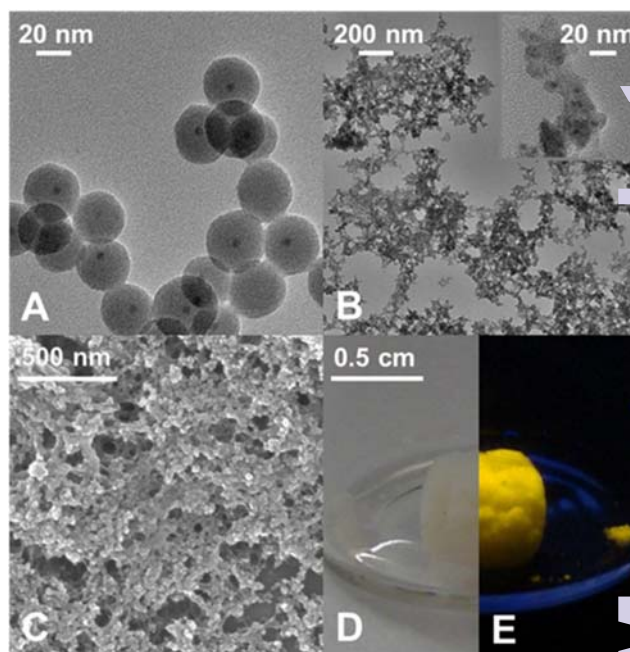


Figure 2: (A) TEM image of ~ 30 nm sized silica nanoparticles with CdSe/CdS QD core. (B) TEM image of silica hydrogel formed out of 20 nm sized silica nanoparticles. After supercritical point drying an aerogel is obtained. (C) SEM image and (D) and (E) a photograph of the solid aerogel under daylight and UV light.

Transmission electron microscopy imaging was done on a LIBRA microscope operating at 200 kV (Carl Zeiss AG). On the beforehand, the samples were prepared by dropping diluted nanoparticle solutions onto a carbon coated copper grid and solvent evaporation. In the case of hydrogels, the sample was sonicated a few seconds before dropcasting.

Scanning electron microscopy (SEM) was performed on a Zeiss DSM 982 Gemini instrument. The samples for SEM characterization were prepared by dropping diluted aerogel dispersions in acetone onto silicon slides and subsequent solvent evaporation.

Nitrogen and carbon dioxide physisorption measurements were performed on an Autosorp 1C (Quantachrome Instruments) using nitrogen (99.999%) and carbon dioxide (99.7%). Specific surface area (SSA) was calculated using the equation from Brunauer, Emmet and Teller (BET) in relative pressure range of 0.05 – 0.20 p/p_0 , and total pore volume was determined at 0.99 p/p_0 . Nonlocal density functional theory (NLDFT) was used to obtain the pore size distribution. Prior to gas physisorption experiments, the sample was activated at 298 K for 48 h under vacuum.

Results and discussion

The gelation mechanism shown here is based on previous results of our group as reported by Lesnyak *et al.* in 2010.¹¹ Using this technique, gels are formed by metal ion assisted complexation of tetrazole capped nanoparticles. This is a fast,

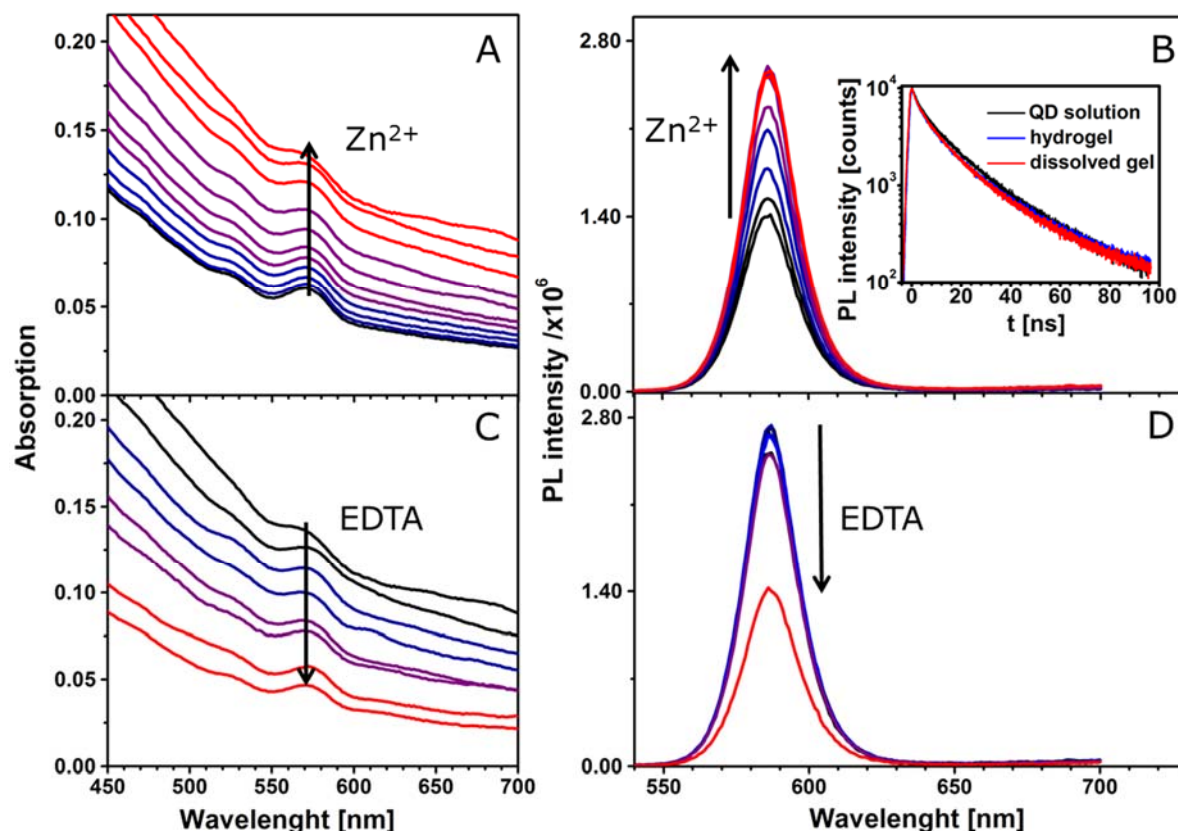


Figure 3: Reversible gel formation monitored by absorption and fluorescence spectroscopy. (A) absorption spectra during gel formation. The stepwise addition of Zn^{2+} ions to the tetrazole capped silica-QDs leads to successive gel formation indicated by the steadily increasing absorption caused by scattering. The corresponding fluorescence spectra (B) meanwhile show an increase of the PL intensity. Since the position of the 1st absorption and the emission maximum do not change during gel formation, it is suggested that the nanocrystals are well separated because of the silica shell and thus do not interact with each other. This also corresponds to the PL decays, inset in (B), where no difference between the QD solution and the hydrogel is observed. (C) and (D) show the absorption and fluorescence spectra during the dissolution of the gel by stepwise addition of EDTA solution. The opposite progress of these spectra compared to (A) and (B) shows the reversibility of this process.

controllable and reversible method to subsequently fabricate 3D networks. The difference here in comparison to the former work, lies in the usage of silica encapsulated QDs instead of bare QDs. The silica shell acts as a spacer between the fluorescent nanocrystals in the three-dimensional network and thus prevents them from quenching, which has been observed before when no spacer was present. Additionally, it provides an option to form hydrogels and aerogels from a broad spectrum of QD materials since our newly developed tetrazole ligand can be applied to any silica coated QD material. The schematic pathway of the 3D assembly of silica encapsulated QDs is shown in Figure 1. In the first step, the QDs are coated with a dielectric shell, in this case silica. Following this, non-classical gel formation is performed by surface capping with tetrazoles and subsequently metal ion addition.

The QDs were encapsulated with silica using a reversed microemulsion technique.³² Details are described in the experimental section. Here we used CdSe/CdS core/shell nanocrystals as a model system to show gel formation and characterization, but we also proved the applicability for other QD materials as will be explained later. The PL QY of the employed QDs was in the region of 30–40%, whereas the PL QY of silica coated QDs was typically between 15–20%. PL QY data for a representative sample are given in Table 1.

The silica shell thickness was varied from 10 to 20 nm in order to efficiently disable coupling between the QDs while preserving a high PL intensity. More information on the influence of the silica shell on the PL of the QDs can be found elsewhere.^{33, 34} An example of silica nanospheres with CdSe/CdS nanocrystal core and an average diameter of 30 nm gives the TEM image in Figure 2 A. According to the image shown, not all silica particles contain QDs. The appearance of silica spheres without QD core is common for most of the reported silanisation procedures. In our case, based on the analysis of several representative TEM images it was not exceeding 5%. After silica coating, the spheres were functionalized with a specially designed tetrazole ligand, 5-(trimethoxysilyl)propylaminomethyl)tetrazole which has the ability to couple to the silica surface via a silane group. Under basic conditions the tetrazole moieties attached to the surface of the silica spheres undergo deprotonation generating negatively charged tetrazolate anions. The latter display a high nucleophilicity and a good coordination potential towards transition metals.^{35, 36} In particular, tetrazolate ligands are known to form stable complexes with Zn^{2+} cations in water. In these complexes, the heteroring exhibits bridging modes through several N atoms

Table 1: Development of the PL QY of a representative sample, starting from bare QDs to silica-QD gel.

Sample	PL QY [%]
CdSe/CdS	31.5
CdSe/CdS@silica	14.1
CdSe/CdS@silica hydrogel	16.8

coordinated to the metal cations which predetermines the networking of nanoparticles by the complexes formed.^{37, 38}

This yields an opportunity to interconnect the particles with the aid of metal ions leading to a 3D structure.³⁹ This non-classical gelation is a controllable and reversible method and has not been applied for silica gels so far. The resulting hydrogel is a very porous non-ordered network as can be seen in the TEM image (Figure 2 B). The network is built up from silica nanospheres which have aligned during the gelation and formed the wirelike 3D assembly. Due to the silica shell, the QDs are well separated from each other in the resulting gel, which has a positive effect on the emission properties as will be discussed below.

In order to obtain a solid material, the hydrogel can be converted into an aerogel by supercritical CO₂ drying. This is a very gentle method to exchange the solvent in the fine pores of the 3D network with air, while maintaining the porous structure and avoiding shrinking of the gel and thus fissures in the material as well as possible. The SEM image in Figure 2 C shows the characteristic sponge-like structure of a silica-QD aerogel produced by this drying procedure. The porous gel structure is preserved during the washing and solvent exchange procedure and the aerogel structure is also robust against moisture due to the high stability of the tetrazole-metal ion complex.

The resulting silica-QD aerogel combines the typical properties of a silica aerogel, e.g. white transparent colour, with those of a QD aerogel. This can be easily seen in the photographs in Figure 2 D and E. Under normal daylight, the aerogel seems to appear as a plain silica gel, still slightly displaying the absorption colour of the QDs, whereas the bright emission colour of the QDs becomes visible when the illumination is changed to UV light.

For the comparison of the silica-QD gel with the pure QD gels, the optical properties of the silica encapsulated QDs have been monitored during the gel formation process by absorption and fluorescence spectroscopy as well as fluorescence lifetime measurements (see Figure 3). Lesnyak *et al.*¹⁵ studied the development of absorption and fluorescence spectra during the gelation and degelation of tetrazole capped CdTe nanocrystals. They reported an increase of absorbance upon gel formation due to increased scattering. The same trend can be observed for the silica-QD gel (see Figure 3 A), meaning that only diffuse reflectance occurs but the absorption properties remain unchanged (see absorption spectrum Figure S1 in supporting information, recorded using an integrating sphere setup). Furthermore, they described a decrease of PL intensity

accompanied by a redshift of the PL maximum and a much faster decay of the PL in the hydrogel due to energy transfer mechanisms. At this point, regarding the PL development in Figure 3 B the advantage of using a spacer to create a defined distance between the nanoparticles becomes very clear. In hydrogels formed from silica encapsulated QDs, the optical properties of the nanoparticles are not changed in comparison to the colloidal solution. The absorption remains unchanged and the PL spectrum does not display a shift of the emission maximum and the PL decay does not change from the colloidal silica-QD solution to the hydrogel, meaning that the applied silica coating successfully avoids energy transfers. Additionally, we observe an apparent increase in PL intensity upon gel formation. However, this increase is not confirmed by PL QY measurements as can be seen from Table 1. This observation is a result solely of the increased emitter concentration induced by the volume contraction during colloid-to-gel transition. The reversibility of this gelation process was demonstrated by the addition of a strong complexing agent, i.e. EDTA, which removes the metal ions from the network and thus initiates degelation. The addition of an equimolar amount of EDTA with respect to the amount of Zn²⁺ leads to complete dissolution of the gel as can be seen from Figure 3 C as decreased scattering. The resulting clear, colloidal solution can restore 100% of the PL intensity of the initial solution.

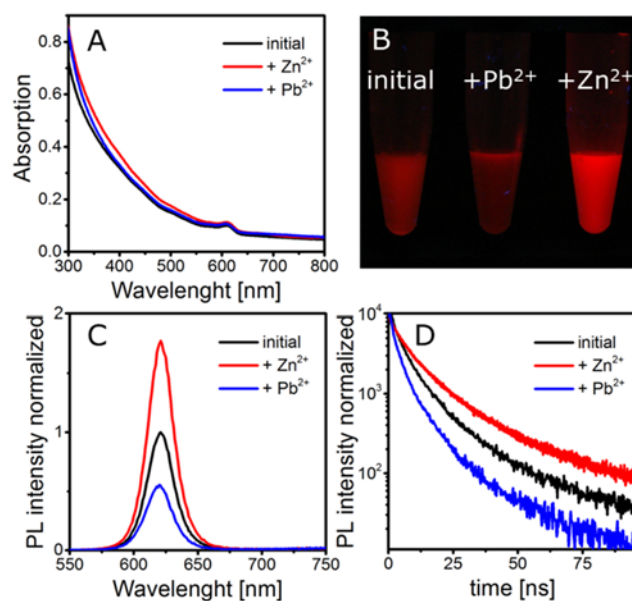


Figure 4: (A) Absorption, (C) fluorescence spectra and (D) PL decay of a silica-QD solution exposed to Zn²⁺ and Pb²⁺. A photograph of the corresponding solutions is shown in (B).

Monitoring the gelation of different charges of silica-QDs analogue to the experiment shown in Figure 3, we observed a different behaviour than explained above when particle batches of lower QY were used. For the gelation of the low QY silica-QDs, Zn²⁺ ions were added to the colloidal solution (for spectroscopy data see Figure S2 in supporting information). The results of the gelation monitoring are in good agreement to those from Figure 3 except for one main difference. Upon stepwise Zn²⁺ ion addition to the colloidal silica-QD solution

healing process is observed before the gelation takes place. The healing is observable as an increase of PL intensity and PL lifetime while the absorption remains unchanged (see Figure 4). When healing is completed, further Zn^{2+} ion addition leads to gel formation with the same characteristics as shown in Figure 3, i.e. increase of PL intensity and absorption due to scattering and unchanged PL lifetime. Subsequently, the addition of an excess amount of EDTA referred to the amount of Zn^{2+} added previously leads to complete gel dissolution. Hence the absorption decreases to the value of the initial colloidal solution. The PL intensity also decreases but only to the value that was reached after healing and the PL lifetime remains unchanged. In short, a permanent healing of the silica-QDs takes place due to the influence of Zn^{2+} ions. From earlier studies we know that the addition of metal ions to QD solutions may lead to surface healing and thus an increase of QY.^{40, 41} However, performing the same experiment using Pb^{2+} instead of Zn^{2+} results in PL quenching (see Figure 4). While absorption is retained, the PL intensity and the PL lifetime of the silica-QDs are reduced in the presence of Pb^{2+} ions. Gels formed with the usage of Pb^{2+} ions show a reduced PL intensity and a faster PL decay compared to the initial solution (for spectroscopy data see Figure S3 in supporting information). Furthermore, this quenching seems to be irreversible since the addition of an excess amount of EDTA does not lead to a recovery of the emission properties.

From this we conclude that the silica shell coated on our QDs is not densely packed but rather porous and allows small species, such as metal ions, to pass through the silica shell to the QD core and hence to interact with the QD surface. In our case, this interaction is observed as a permanent enhancement of the PL intensity and lifetime in the case of Zn^{2+} and a decrease of the PL intensity and lifetime in the case of Pb^{2+} .

According to the literature, silica shells are expected to act as a protecting layer to prevent the QDs from photodegradation and impede the release of heavy metal ions.^{42, 43}

However, several studies confirmed the existence of a certain porosity in the examined silica shells. Although no indication of porosity is given by high-resolution TEM, the existence of micro- and mesoporous cavities in colloidal silica particles was observed in BET gas adsorption isotherms.^{44, 45} Liz-Marzán and Mulvaney showed for glass coated Ag nanoparticles grown with sodium silicate that the shells are porous and the core can undergo a variety of chemical reactions.⁴⁶ The reaction rate thereby is reduced with increasing shell thickness, but even for the largest shell thickness of 23 nm, the reaction was not negligible. The porous nature has also been reported for sol-gel derived silica spheres.⁴⁷ However, it should be mentioned that the porous structure strongly depends on the preparation and cleaning conditions as well as on the shell thickness⁴⁸ and might therefore vary between different preparation techniques.

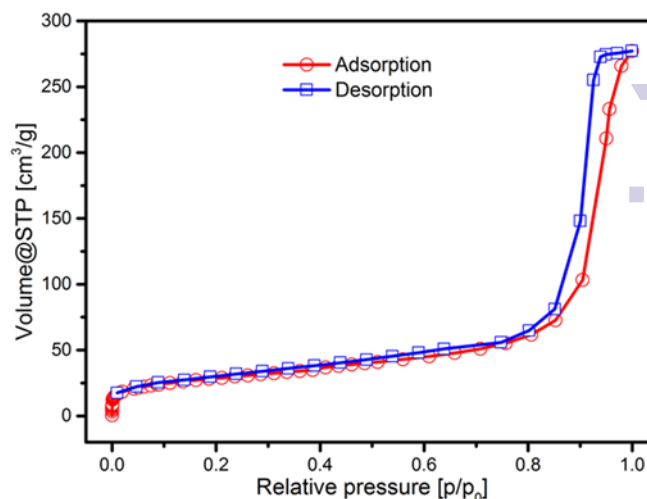


Figure 5: Nitrogen adsorption (at 77K) isotherm of microemulsion derived silica nanoparticles with average diameter of 42 nm

To prove the porosity of our silica particles derived by the microemulsion approach, we determined the specific surface area using nitrogen physisorption measurement at 77 K. The adsorption isotherm is presented in Figure 5. In the range of 10^{-6} up to 0.8 p/p_0 , the isotherm matches well with the type I isotherm that is specific for microporous materials according to IUPAC classification. The strong increase at higher relative pressure ($> 0.8 p/p_0$) is referred to the filling of interparticle pores with nitrogen molecules. The BET specific surface area (SSA) was determined to be $102 \text{ m}^2/\text{g}$, which is higher compared to the theoretical geometric surface area of the silica nanoparticles of $75.2 \text{ m}^2/\text{g}$, supporting the existence of a certain porosity. The geometric surface area was determined using the average external diameter of the spheres from TEM of 42 nm and a bulk density of $1.9 \text{ g}/\text{cm}^3$.⁴⁷ The pore size distribution from the NLDFT model exhibits pore widths within the range of micro- and mesopores (see Figure S4 supporting information). The measurement of carbon dioxide adsorption at 273 K allows a more detailed statement about the microporosity of the material. In Figure S4 C the CO_2 isotherm in the range of 10^{-4} up to $3 \times 10^{-2} p/p_0$ is shown, which presents the adsorption in micropores. A micropore volume of $0.11 \text{ cm}^3/\text{g}$ was determined, indicating a good porosity of the silica material.

This porosity might be useful with respect to future sensing applications of the material. As shown before, the PL properties are sensitive towards metal ions. This concentration dependent influence of metal ions (see Figure S2 and S3) makes them a promising ion sensing material. The porosity of the material is therefore a necessary requirement to provide the transport of the analyte from the outer media to the QD core.

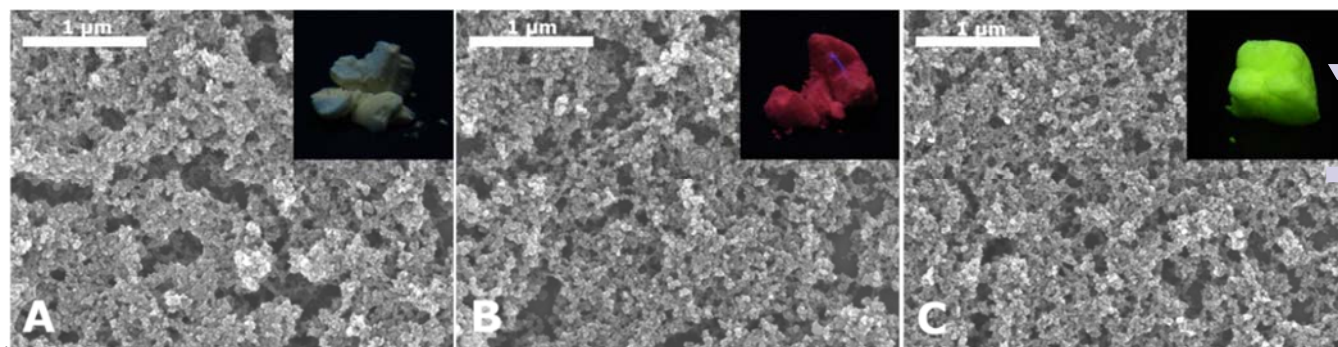


Figure 6: SEM images and photographs (insets) of silica aerogels with different QD cores. The QD cores are (A) In(Zn)P/GaP/ZnS, (B) CdSe/CdS/ZnS and (C) a CdSe/ZnS alloy.

The gelation method shown here is applicable to any silica coated nanoparticle material. We performed the same procedure not only with CdSe/CdS QDs but also with three other QD materials, namely In(Zn)P/GaP/ZnS, CdSe/CdS/ZnS and a CdSe/ZnS alloy. Figure 6 shows SEM images and photographs under UV light of the aerogels produced from these materials. As can be seen from the photographs, the PL intensities of the aerogels made from different materials differ significantly. This is caused by two main reasons: (i) the differing QY from the different QD materials and (ii) PL losses during silica coating. Especially the second aspect is very disadvantageous. We assume that additional trap states are formed on the QD surface during the silica coating procedure, e.g. caused by ligand exchange of the organic ligands with partially hydrolysed TEOS.^{17, 18, 34} The extent of PL loss was observed to be lower for core/shell QDs with several monolayers of shell material compared to bare QD cores, but can differ between different QD batches.

The possibility to produce 3D networks from silica coated QDs with different QD core materials simultaneously opens the opportunity to produce a variety of mixed structures, since similar surface chemistry is provided by the silica shell and the attached tetrazole ligand. Mixing for example two differently emitting silica-QD species provides a very easy possibility to tune the colour of the resulting gel. Since energy transfer is disabled in this architecture due to the large distance between the emitting species, no spectral shifts have to be considered when mixing the desired emission colour. This can be demonstrated in the following experiment. Figure 7 A shows a photograph of two differently emitting silica-QD species, i.e. QD1 and QD2 and mixtures of both species, i.e. Mix1-Mix3, in different ratios in colloidal solution and as hydrogels. As expected, the emission colour in solution and in the gel is identical. This observation is supported by the fluorescence spectra of the solutions and the corresponding gels (see Figure 7 B). No spectral shifts or significant changes of the peak area ratios are observed for all three mixtures in solution and in the gel. Thanks to this, the colour of the mixed gel can be easily tuned. The diagram in Figure 7 C demonstrates that subsequent increasing of the red component equivalently shifts the colour of the mixture providing the possibility to create different shades of yellow.

Conclusions

We have developed a new aerogel material with no PL quenching behaviour from silica encapsulated semiconductor QDs, based on a method reported for colloidal solutions of semiconductor and metal nanoparticles. In comparison to other monolithic silica-QD structures, we supply a defined and controllable distance between the QDs in our gel, providing control over energy transfer processes. Silica encapsulation has been done by using a well-known reverse microemulsion approach that allows uniform and controllable shell formation. In order to perform reversible gel formation we developed a new tetrazole ligand that was intentionally designed to specifically bind to the silica surface. Facile 3D assembly of silica-QDs capped with this ligand was achieved by metal ion complexation of the negatively charged tetrazole rings. By monitoring the gel formation process with optical spectroscopy, we were able to show, that the optical properties of the nanocrystals could be preserved in the 3D network. No spectral shifts, lifetime shortening, PL quenching or decrease of PL QY is observed in this novel gel material, as until now has all along been the case for these kind of gels prepared from non-coated QDs. Using nitrogen and carbon dioxide physisorption measurements, we showed that the silica shell is porous and allows metal ions, such as Zn²⁺ and Pb²⁺ to pass through the shell and interact with the QD core causing detectable changes of the emission properties. This makes them a promising material for metal ion sensing application. We further showed the applicability of this gelation method to other QD materials which sets the stage for facile preparation of a variety of mixed gel structures. With respect to future applications in the field of solid state lighting, we showed the advantage of the architecture of our aerogel for colour tuning. As an example, we demonstrated on the basis of two differently emitting silica-QD species that colour tuning of the resulting mixed gel is very straightforward because no energy transfer and thus no spectral shifts have to be considered.

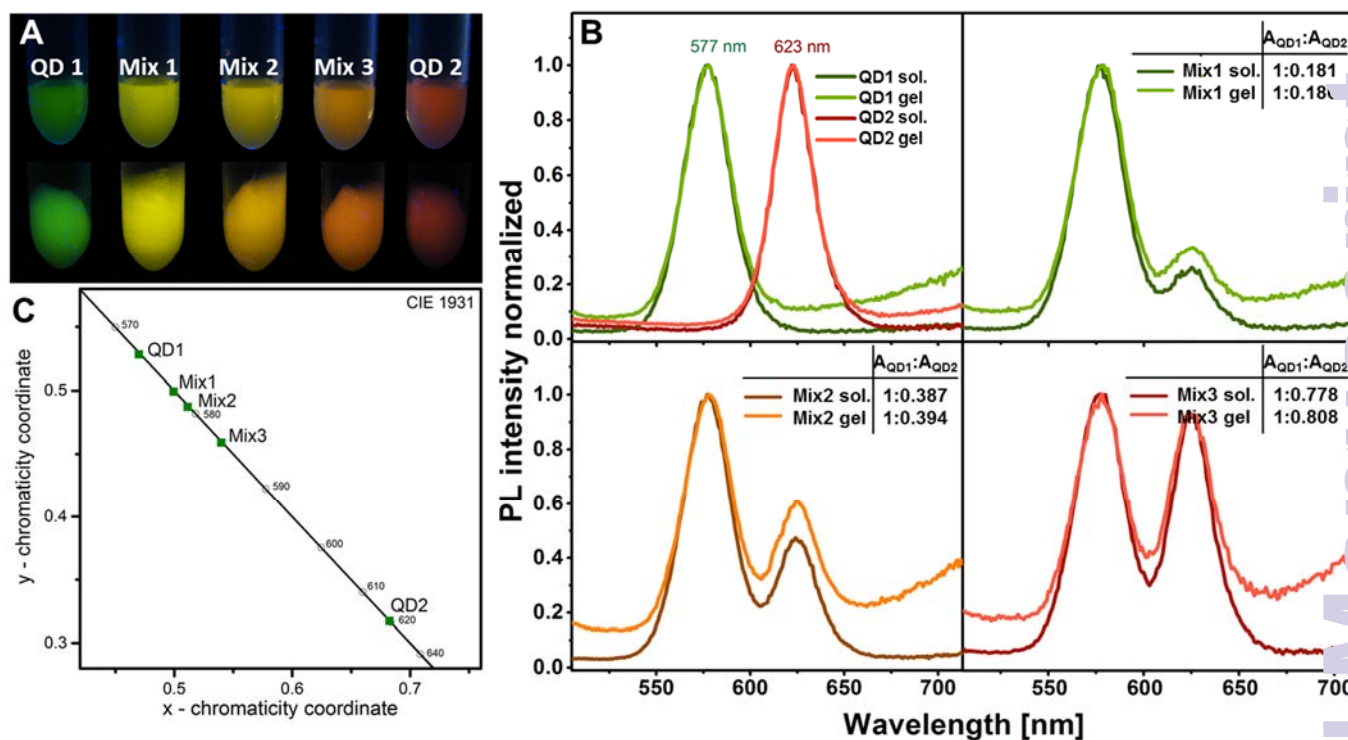


Figure 7: (A) Photograph of two differently emitting silica-QDs and mixtures of both species in differing ratios in solution (upper row) and as hydrogels (lower row). The emission colours are not changed in the hydrogel compared to the solution, since energy transfer from donor particles to acceptor particles is disabled due to the large distance between both species. (B) Fluorescence spectra of two differently emitting silica-QDs and mixtures of both species in differing ratios in solution and hydrogels. The optical properties of the initial solutions are preserved in the gel as can be seen from the comparison of the peak area ratios $A_{QD1}:A_{QD2}$ of both species. (C) CIE (Commission internationale de l'éclairage) coordinates of the two differently emitting silica-QDs and their mixtures.

Acknowledgements

This work was supported by DFG project EY16/10-2, the European Research Council (ERC-2013-AdG project AEROCAT) and the EU FP7 Network of Excellence "Nanophotonics for Energy Efficiency". S.V. gratefully acknowledges the European Science Foundation for the exchange grant within ESF activity "New Approaches to Biochemical Sensing with Plasmonic Nanobiophotonics (PLASMON-BIONANONSENSE)". Special thanks to Zoran Popović for imparting of knowledge of silica coating.

Notes and references

- N. Hüsing and U. Schubert, *Angew. Chem., Int. Ed.*, 1998, **37**, 22-45.
- S. S. Kistler, *Nature*, 1931, **127**, 741-741.
- H. D. Gesser and P. C. Goswami, *Chem. Rev. (Washington, DC, U. S.)*, 1989, **89**, 765-788.
- N. C. Bigall, A.-K. Herrmann, M. Vogel, M. Rose, P. Simon, W. Carrillo-Cabrera, D. Dorfs, S. Kaskel, N. Gaponik and A. Eychmüller, *Angew. Chem., Int. Ed.*, 2009, **48**, 9731-9734.
- V. Lesnyak, A. Wolf, A. Dubavik, L. Borchardt, S. V. Voitekhovich, N. Gaponik, S. Kaskel and A. Eychmüller, *J. Am. Chem. Soc.*, 2011, **133**, 13413-13420.
- S. Bag, I. U. Arachchige and M. G. Kanatzidis, *J. Mater. Chem.*, 2008, **18**, 3628-3632.
- S. Bag, P. N. Trikalitis, P. J. Chupas, G. S. Armatas and M. G. Kanatzidis, *Science*, 2007, **317**, 490-493.
- I. U. Arachchige and S. L. Brock, *J. Am. Chem. Soc.*, 2007, **129**, 1840-1841.
- I. U. Arachchige and S. L. Brock, *Acc. Chem. Res.*, 2007, **40**, 801-809.
- I. U. Arachchige and S. L. Brock, *J. Am. Chem. Soc.*, 2006, **128**, 7964-7971.
- A. Eychmüller, *Angew. Chem.*, 2005, **117**, 4917-4919.
- N. Gaponik, A. Wolf, R. Marx, V. Lesnyak, K. Schilling and A. Eychmüller, *Adv. Mater.*, 2008, **20**, 4257-4262.
- J. L. Mohanan, I. U. Arachchige and S. L. Brock, *Science*, 2005, **307**, 397-400.
- T. Hendel, V. Lesnyak, L. Kühn, A.-K. Herrmann, N. C. Bigall, L. Borchardt, S. Kaskel, N. Gaponik and A. Eychmüller, *Adv. Funct. Mater.*, 2013, **23**, 1903-1911.
- V. Lesnyak, S. V. Voitekhovich, P. N. Gaponik, N. Gaponik and A. Eychmüller, *ACS Nano*, 2010, **4**, 4090-4096.
- S.-Y. Chang, L. Liu and S. A. Asher, *J. Am. Chem. Soc.*, 1999, **121**, 6739-6744.
- M. Darbandi, R. Thomann and T. Nann, *Chem. Mater.*, 2005, **17**, 5720-5725.

18. R. Koole, M. M. van Schooneveld, J. Hilhorst, C. de Mello Donegá, D. C. 't Hart, A. van Blaaderen, D. Vanmaekelbergh and A. Meijerink, *Chem. Mater.*, 2008, **20**, 2503-2512.
19. C. Graf, D. L. J. Vossen, A. Imhof and A. van Blaaderen, *Langmuir*, 2003, **19**, 6693-6700.
20. Y. Kobayashi, T. Nozawa, T. Nakagawa, K. Gonda, M. Takeda, N. Ohuchi and A. Kasuya, *J. Sol-Gel Sci. Technol.*, 2010, **55**, 79-85.
21. M. A. Correa-Duarte, M. Giersig and L. M. Liz-Marzán, *Chem. Phys. Lett.*, 1998, **286**, 497-501.
22. W. Stöber, A. Fink and E. Bohn, *J. Colloid Interface Sci.*, 1968, **26**, 62-69.
23. H. Yamauchi, T. Ishikawa and S. Kondo, *Colloids Surf.*, 1989, **37**, 71-80.
24. K. Osseo-Asare and F. J. Arriagada, *Colloids Surf.*, 1990, **50**, 321-339.
25. C.-L. Chang and H. S. Fogler, *Langmuir*, 1997, **13**, 3295-3307.
26. Q. Wang, N. Iancu and D.-K. Seo, *Chem. Mater.*, 2005, **17**, 4762-4764.
27. S. Jun, J. Lee and E. Jang, *ACS Nano*, 2013, **7**, 1472-1477.
28. C. Li and N. Murase, *Langmuir*, 2004, **20**, 1-4.
29. P. Yang, C. L. Li and N. Murase, *Langmuir*, 2005, **21**, 8913-8917.
30. L. Sorensen, G. F. Strouse and A. E. Stiegman, *Adv. Mater.*, 2006, **18**, 1965-1967.
31. Y. Chan, P. T. Snee, J.-M. Caruge, B. K. Yen, G. P. Nair, D. G. Nocera and M. G. Bawendi, *J. Am. Chem. Soc.*, 2006, **128**, 3146-3147.
32. Z. Popović, W. Liu, V. P. Chauhan, J. Lee, C. Wong, A. B. Greytak, N. Insin, D. G. Nocera, D. Fukumura, R. K. Jain and M. G. Bawendi, *Angew. Chem., Int. Ed.*, 2010, **49**, 8649-8652.
33. Y. Ma, Y. Li, S. Ma and X. Zhong, *Journal of Materials Chemistry B*, 2014, **2**, 5043-5051.
34. P. Yang, M. Ando and N. Murase, *Langmuir*, 2011, **27**, 9535-9540.
35. P. N. Gaponik, S. V. Voitekhovich and O. A. Ivashkevich, *Russ. Chem. Rev.*, 2006, **75**, 507-539.
36. G. Aromí, L. A. Barrios, P. Gamez and O. Roubeau, *Coord. Chem. Rev.*, 2011, **255**, 485-546.
37. H. Zhao, Z.-R. Qu, H.-Y. Ye and R.-G. Xiong, *Chem. Soc. Rev.*, 2008, **37**, 84-100.
38. L. Ma, Y.-C. Qiu, G. Peng, J.-B. Cai and H. Deng, *Eur. J. Inorg. Chem.*, 2011, DOI: 10.1002/ejic.201100213, 3446-3453.
39. J. H. Lee, H. Lee, S. Seo, J. Jaworski, M. L. Seo, S. Kang, J. Y. Lee and J. H. Jung, *New J. Chem.*, 2011, **35**, 1054-1059.
40. H. H.-Y. Wei, C. M. Evans, B. D. Swartz, A. J. Neukirch, J. Young, O. V. Prezhdo and T. D. Krauss, *Nano Lett.*, 2012, **12**, 4465-4471.
41. A. Wolf, V. Lesnyak, N. Gaponik and A. Eychmüller, *J. Phys. Chem. Lett.*, 2012, **3**, 2188-2193.
42. Y. Yang, L. Jing, X. Yu, D. Yan and Gao, *Chem. Mater.*, 2007, **19**, 4123-4128.
43. P. Yang, M. Ando and N. Murase, *J. Colloid Interface Sci.*, 2007, **316**, 420-427.
44. A. van Blaaderen and A. P. M. Kentgens, *J. Non-Cryst. Solids*, 1992, **149**, 161-178.
45. A. van Blaaderen and A. Vrij, *J. Colloid Interface Sci.*, 1993, **156**, 1-18.
46. T. Ung, L. M. Liz-Marzán and P. Mulvaney, *Langmuir*, 1997, **14**, 3740-3748.
47. S. Li, Q. Wan, Z. Qin, Y. Fu and Y. Gu, *Langmuir*, 2014, **30**, 824-832.
48. P. Yang and N. Murase, *ChemPhysChem*, 2010, **11**, 815-821.